PH-dependent photochemical transformation of arsenic sulfide sludge accelerated by visible light irradiation: the catalytic oxidation mechanism of ferric ions

Hongbo Lu,[†,¶] Chunli Wang,[†] Xueming Liu,[‡] Jing Zhang,[†,¶] Zhang Lin,[‡] Zhengping Hao,[¶] Gang Pan[⁑]

[†] Key Laboratory of Environmental Nano-technology and Health Effect, Research Center for Eco-Environmental Sciences, Chinese Academy of Sciences, Beijing 100085, P. R. China

[¶] National Engineering Laboratory for VOCs Pollution Control Materials & Technology, University of Chinese Academy of Sciences, Beijing 101408, P.R. China

[‡] School of Environment and Energy, South China University of Technology, Guangzhou 510006, P.R. China

[⁑] Centre of Integrated Water-Energy-Food Studies (*i*WEF), School of Animal, Rural, and Environmental Sciences, Nottingham Trent University, Brackenhurst Campus, NG25 0QF, UK

ABSTRACT:

The fate of arsenic sulfide sludge (ASS), a typical precipitation product of acid smelting wastewater, is readily affected by the surrounding conditions when deposited in environment. When exposed to sunlight, the dissolution and oxidation of ASS were markedly accelerated. However, the photocatalytic transformation mechanism of ASS is still unclear. Herein, the release and oxidation of As(III) in ASS under visible light was investigated by employing artificial arsenic sulfide with Fe(II)/Fe(III) ions. Results show that the coexisting ferric ions are critical to promote the photo-oxidation of As(III) released from the parental solid into As(V). The photo-oxidation rate can reach 149 μM/h in the presence of 0.5 mM Fe(II) ions at pH 1.3, ~5 times of that in the absence of Fe(II). The pH-dependent mechanism of photocatalytic oxidation of As(III) stimulated by Fe(II) ions is proposed and verified. In acid conditions (pH 1.3 and 3), photo-generated hydroxyl and sulfate radicals were promoted by Fe(II)/Fe(III) cycling catalysis with the assistance of the reductive sulfur species from ASS, e.g. S^{2-} and SO_3^{2-}, and thus accelerated the oxidation of As(III). While at pH 7, the nascent ferric hydroxide colloids enhanced the oxidation rate of As(III) via photo-induced ligand-to-metal-charge transfer (LMCT) mechanism. These findings can help in predicting and controlling the fate of real arsenic-containing sludge in sunlit environments.

KEYWORDS: Arsenic sulfide sludge, As(III) oxidation, photo-catalysis, iron ions

Graphical abstract:

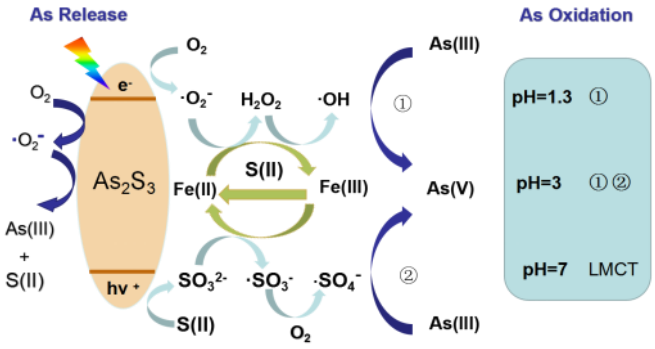

Introduction

Arsenic is of particular environmental concern due to its carcinogenic toxicity, which has become a worldwide issue of public health.[1] Arsenic contamination has mainly come from anthropologic activities. Especially, during metal smelting and mineral processing, a large amount of acid wastewater (pH<2) is produced, which contains a high concentration of arsenic, together with other metal ions, such as iron, copper.[2,3] In industry, sulfide precipitation is commonly used for treatment of arsenic-containing acid wastewater, owing to its higher precipitation efficiency at the low pH condition and smaller volume of sludge produced.[4-6] As a result, large quantities of arsenic sulfide sludge (ASS) with a low pH (< 2) are discharged into environment. When deposited in the environment, ASS is susceptible to natural environmental factors, such as pH, temperature and dissolved oxygen.[7-9] For example, the dissolution rates of artificial arsenic sulfide at the higher pH values, are in the range of 26–4478 times relative to those at pH 2.[10]

Similar to the photochemical transformation of natural minerals (e.g. Fe- and Mn-oxides),[11] sunlight also has a profound impact on the fate of ASS deposited in the environment. Our recent study found that sunlight can not only accelerate the dissolution of ASS to release As(III) ions, but also markedly increase the oxidation rate of As(III) into As(V).[12] In ASS, the main component, As_2S_3, is viewed to act as the photo-responsive semiconductor to generate active oxygen free radicals under light irradiation (eqs. 1-4), which will adversely affect the stability of the host solid particles and cause the dissolution and oxidation of ASS (eqs. 5-6).[12]

$$ASS + h\nu \rightarrow e_{cb}^{-} + h_{vb}^{+} \quad (1)$$

$$O_2 + e_{cb}^{-} \rightarrow \bullet O_2^{-} \quad (2)$$

$$\bullet HO_2 + \bullet O_2^{-} + H^{+} \rightarrow H_2O_2 + O_2 \quad (3)$$

$$H_2O_2 + h\nu \rightarrow 2\bullet OH \quad (4)$$

$$ASS + \bullet O_2^{-} + H^{+} \rightarrow 3\bullet S^{-} + HO_2^{-} + 2As(III) \quad (5)$$

$$As(III) + \bullet OH \rightarrow As(V) + OH^{-} \quad (6)$$

However, the reported result from ASS is quite different to the photo-erosion of the synthetic arsenic sulfide, where only the release of As(III) ions has been observed.[13] The difference could be reasonably ascribed to the fact that in the real ASS, the solid sludge normally contains As_2S_3 co-existing with other inorganic metal ions of impurities, such as ferric and copper ions, depending on the different smelting processing.[2,3] These incorporated ions might affect the photochemical reaction in ASS.

It has been discussed that ferric ions, especially Fe(II), could trigger the active oxygen species to oxide As(III) into As(V) ions in aqueous solution, both with and without light irradiation. For example, in the presence of 0.06-5 mg/L Fe(II, III) at pH 6.5-8.0, As(III) is partly oxidized in the dark, while over 90% of As(III) is oxidized within 2-3 h under 90 W/m^2 UV light.[14] The promotion of As(III) oxidation rate can be attributed to the photo-generated •OH. Moreover, the arsenic oxidation can also be accelerated by the addition of sulfite to produce sulfate radicals under light irradiation.[15] While in the neutral condition, the formation of As(III)-Fe(II) complex plays a critical role in the oxidation of As(III) by promoting the production of H_2O_2.[16]

Similarly, the As(III) oxidation can be realized on colloidal ferric hydroxide (CFH) under light illumination, through electron transfer from As(III) to Fe(III) by ligand-to-metal-charge transfer (LMCT) mechanism.[17] In addition to the oxidation of As(III) ions in solution, the co-existence of Fe(III) or Fe(II) ions can also accelerate the transformation of As-containing solids. It has been reported that the dissolution of arsenopyrite (FeAsS) minerals could be elevated by the oxidation effect of Fe(III) directly.[18] For arsenic-bearing tailings (realgar and pharmacolite), Fe(II)-excited active oxygen species such as hydroxyl radicals, superoxide or hydrogen peroxide, increased the dissolution and oxidation rate of arsenic in the slag, and subsequently formed more stable Fe-As complex or minerals.[19] Although the effect of Fe ions acting on the transformation of As species has been reported, no studies has examined the coupling effects of light irradiation and Fe ions on the fate of ASS in the environment. In this work, the specific role of ferric ions in the photochemical dissolution and oxidation of ASS was systematically studied by adding Fe(II) into the artificial arsenic sulfide under visible light, with the aim to understand the light-induced transformation mechanism of real ASS, which is different to the pure arsenic sulfide (As_2S_3). The release and oxidation kinetics of As_2S_3 were investigated at different pHs under visible light. The photo-generated active oxygen and sulfur species were identified by EPR and free radical quenching experiments, and their specific contributions to the transformation of the sludge are discussed. The photocatalytic oxidation mechanism of As(III) in ASS was proposed on the basis of the analysis of Fe(II)/Fe(III) cycling in the Fe-As_2S_3 system. The present work will

help to understand the photo-induced transformation behavior of arsenic-containing sludge deposited in sunlit environments.

2. Experimental Section

2.1. Chemicals.

H_2SO_4 (GR), Fe(II) ($FeSO_4$•$7H_2O$, AR), Fe(III) ($Fe_2(SO_4)_3$•xH_2O, AR), ascorbic acid (AR), $C_4H_4KO_7Sb$•$0.5H_2O$ (CP) were purchased from Sinopharm Chemical Reagent Co. Ltd. *Tert*-Butyl alcohol (TBA, AR) and methanol (MeOH, AR) were purchased from Shanghai Shiyi Chemicals Reagent Co. Ltd. 5,5-dimethyl-1-pyrroline-N-oxide (DMPO) and Na_2S•$9H_2O$ (AR) were purchased from Internet Aladdin Reagent Database Inc. (Shanghai, China). $NaAsO_2$ was purchased from Sigma-Aldrich. Deionized (DI) water was used for all experiments without further purification.

2.2. Synthesis of As_2S_3.

Under vigorous magnetic stirring, 30 mL Na_2S solution (1.2 M) were added into 60 mL $NaAsO_2$ solution (0.4 M), and H_2SO_4 was used to keep pH in the range of 1.8-2. The formed suspension was continuously stirred for 10 min, and then washed with deionized water. The suspension was filtrated and dried at 60 ^oC for 2 d.

2.3. Photo Reaction System.

All the photo reactions were conducted in a 250 mL beaker with 0.6 $g \cdot L^{-1}$ As_2S_3 powder. A 500-W Xe arc lamp (Shanghai Jiguang Special Lighting Appliance Factory, China) was used as the light source ($\lambda > 420$ nm) and placed approximately 20 cm

above the beaker. A water-cooling system was used to keep the room temperature (RT, ~25 ^{o}C) for all reactions. At the appropriate time interval, sample aliquots were taken out and filtered through a 0.25 μm filter to remove solid particles for further analysis. In order to study the effect of active free radical species, 0.1 M tert-butyl alcohol (TBA) (for scavenging •OH)[20] and 0.1 M methanol (for both $\bullet SO_4^-$ and •OH)[21] were used as the quencher and added in the photo-reaction system.

2.4. Analytical Methods.

2.4.1. Arsenic, iron and sulfur species in the liquid phase

The concentrations of As(V) and total arsenic (TAs) were analyzed using the colorimetric molybdene blue method.[22] Sulfur species, including S(II) and S(IV), were measured using the methylene blue method at 660 nm[23] and a modified colorimetric procedure with DTNB at 412 nm[24] by an UV−vis spectrophotometer. The concentration of SO_4^{2-} was obtained on an ion chromatograph (IC, Dionex Aquion 112018-0141, USA) with a Dionex IonPac AS 19 (4 ×250 mm) column and a conductivity detector. The concentration of Fe(II) was determined using a colorimetric complexant (1,10-phenanthroline) at 510 nm, and the total Fe ions (TFe) were measured after Fe(III) ions were completely reduced by hydroxylamine hydrochloride.[25]

2.4.2. Solid phase of As_2S_3

The morphology of solid samples was characterized on a scanning electron microscopy (SEM, SU8020, Japan). The crystal structure of samples was recorded on an X-ray diffraction (XRD, PANalytical B.V.X'Pert3 Powder) with a Cu−K(alpha)

source at 40 kV with 40 mA. X-ray photoelectron spectroscopy (XPS) was performed on an ESCALAB 250Xi instrument (Thermo Fisher Scientific).

2.4.3. EPR analysis of active free radicals

•OH and $\bullet SO_4^-$ radicals were detected on a Bruker EleXsys EPR spectrometer (A300-10/12, Germany) at 25 ^oC using DMPO as the scavenger.

Results and discussion

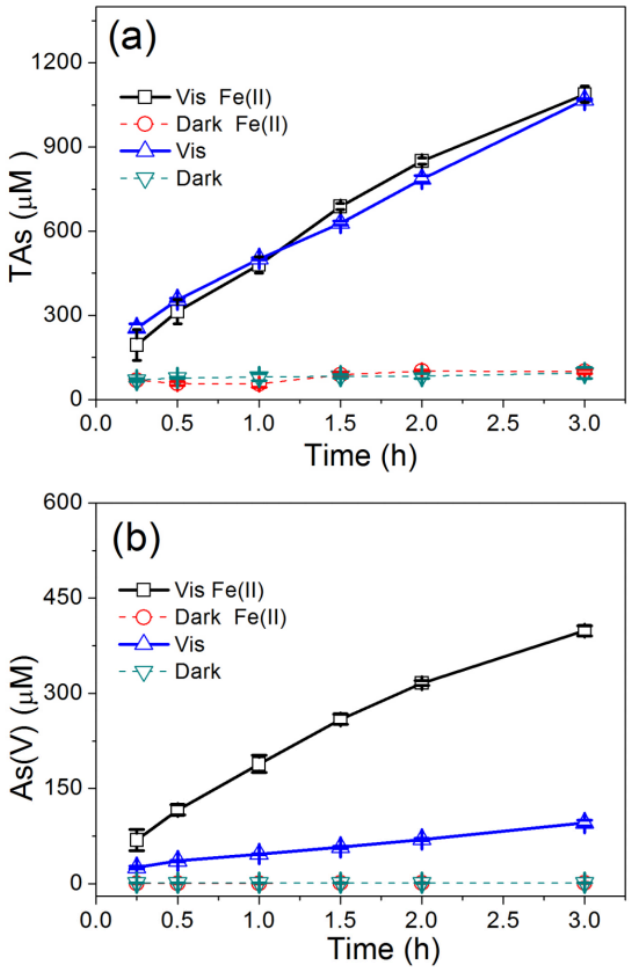

Fig. 1. Effect of visible light (vis) on the release (TAs) (a) and oxidation (As(V)) (b) of arsenic in As_2S_3 with 1 mM Fe(II) at pH 1.3.

Release and oxidation of arsenic in the Fe(II)-As_2S_3 system under visible light. The as-synthesized As_2S_3 had an amorphous structure with the particle size of ~ 100 nm (See XRD and SEM in Fig S1). As(III) and S(II) were the main components of solid, with the ratio of 2:3, as confirmed by XPS and EDS in Fig S1. The results are similar to the real arsenic sludge by sulfide precipitation in our previous study.[12]

The concentrations of TAs and As(V) were monitored in Fe(II)-As_2S_3 system at different pHs (1.3, 3 and 7), to evaluate the release and oxidation of As(III) under visible light, respectively. As shown in Fig. 1a-b and Fig. S2, in the dark only a very small amount of arsenic ions (67 μM at t=3 h) was released from As_2S_3 without Fe(II) at pH 1.3, which slightly increased with pH. However, no As(V) was produced from the oxidation of As(III). Moreover, the addition of Fe(II) increased neither the release nor the oxidation of arsenic ions at acid conditions. At pH 7 (Fig. S2c), the concentration of TAs decreased slightly with the increase of Fe(II), which might be due to the adsorption or co-precipitation by nascent colloidal ferric hydroxide (CFH).[26]

Under visible light, an obvious release (TAs) of arsenic together with a slight arsenic oxidation (As(V)) were observed in As_2S_3 system without Fe(II). The release rate of TAs markedly increased to 362 μM/h at pH 1.3 (Fig. 1a), but the addition of Fe(II) had little effect on the release of arsenic ions from As_2S_3 (Fig. 1a and Fig. S3). However, the production of As(V) greatly increased in the presence of Fe(II), and the oxidation rate of As(III) into As(V) was linearly fit to be 132 μM/h in 1.0 mM Fe(II) solution at pH 1.3, which is 4.2 times higher than that in the absence of Fe(II). The

results confirmed the effect of Fe(II) on accelerating the photo-oxidation of the released As(III). The oxidation rate increased with the increase of Fe(II) concentration at all the three pHs (Fig. 2a-c), but decreased with the pH values (Table S1 and Fig. S4). In short, Fe(II) had no effect on the release of As(III) ions from As_2S_3 under visible light, but markedly accelerated the photo-oxidation of the released As(III) into As(V).

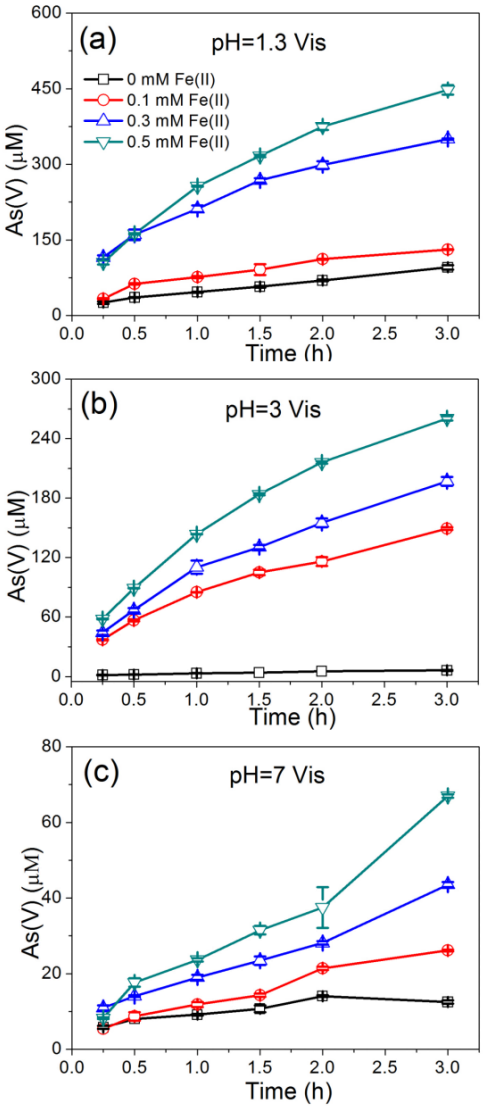

Fig. 2. Arsenic oxidation of As_2S_3 in the presence of Fe(II) at pH 1.3 (a), 3 (b), and 7 (c) under visible light.

Sulfur species in the system of Fe(II)-As_2S_3. During the photochemical reaction of As_2S_3, sulfur species in Fe(II)-As_2S_3 system were also monitored. As shown in Fig. 3a-b, the main sulfur specie in the solution at pH 1.3 and 3 was SO_4^{2-}, and no S(II) was detected at both pHs. Instead, S(II) was dominant in solution at pH 7 and little SO_4^{2-} was observed. The results suggest that during the photochemical reaction of As_2S_3, S(II) species that originally released from the solid were almost oxidized into SO_4^{2-} in acid conditions, but the oxidation was suppressed in the neutral solutions. It is worthy of noting that no intermediate sulfur species, e.g. SO_3^{2-} was detected at all three pH values.

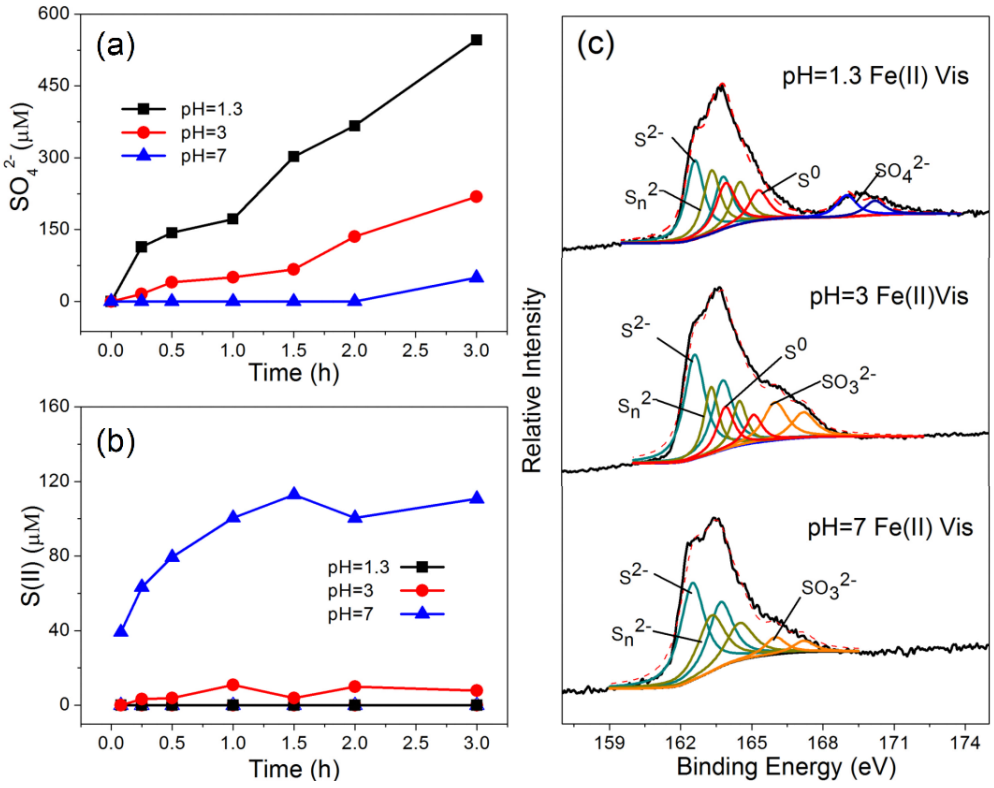

Fig. 3. (a-b) Release rates of different sulfur species (SO_4^{2-} and S(II)) in 1mM Fe(II) solution under visible light irradiation. (c) XPS spectra of S 2p for As_2S_3 in the presence of 1 mM Fe(II) after 3 h visible light irradiation at pH 1.3, 3, and 7.

The sulfur species on the As_2S_3 solid particles after visible light irradiation were

further characterized by XPS. Before illumination, only two group peaks corresponding to S^{2-} and S_n^{2-} occurred (Fig. S1c). But after light irradiation, S 2p XPS spectra were significantly changed at three different pH values. As shown in Fig. 3c, the peaks from 161 to 170 eV are corresponding to S 2p, which can be fitted by five groups of peaks. Each group with a separation of 1.19 eV and intensity ratio of 2:1, is assigned to S $2p_{3/2}$ and S $2p_{1/2}$.[27] These five group peaks located at the binding energies of 162.6-163.79 eV, 163.3-164.49 eV, 163.9-165.09 eV, 166.0-167.19 eV, and 169.0-170.19 eV are assigned to S^{2-}, S_n^{2-}, S^0, SO_3^{2-}, and SO_4^{2-}, respectively.[28-30] It can be clearly seen that SO_4^{2-} was obtained on the surface of solid particles at pH 1.3, while disappeared at pH 3 and 7. Instead, SO_4^{2-} was replaced by SO_3^{2-} appearing at both the higher pHs. It indicated that during the photochemical reaction, the oxidation of sulfur decreased with the increase of pH values. This can be further confirmed by the production of S^0, which had a higher ratio at a lower pH and almost not produced at pH 7 (See the fitting results in Table S2).

The solid production of S^0 was further verified by XRD analysis of the collected As_2S_3 samples after photochemical reactions (Fig. S5). After illumination, the new sharp diffraction peaks of S_8 were clearly observed at acidic conditions (pH 1.3 and 3), which were more pronounced in the O_2-saturated conditions the enhanced release and oxidation of arsenic (Fig. S6). After 3 h irradiation, a thin layer of yellow solid, hydrophobic S_8, was visibly formed to float on the surface of the solution (Fig. S7). The results confirmed that during the photochemical reaction, most of sulfide ions in As_2S_3 were transformed into sulfur solid, which could provide the possibility for the

subsequent recycle of sulfur resource.

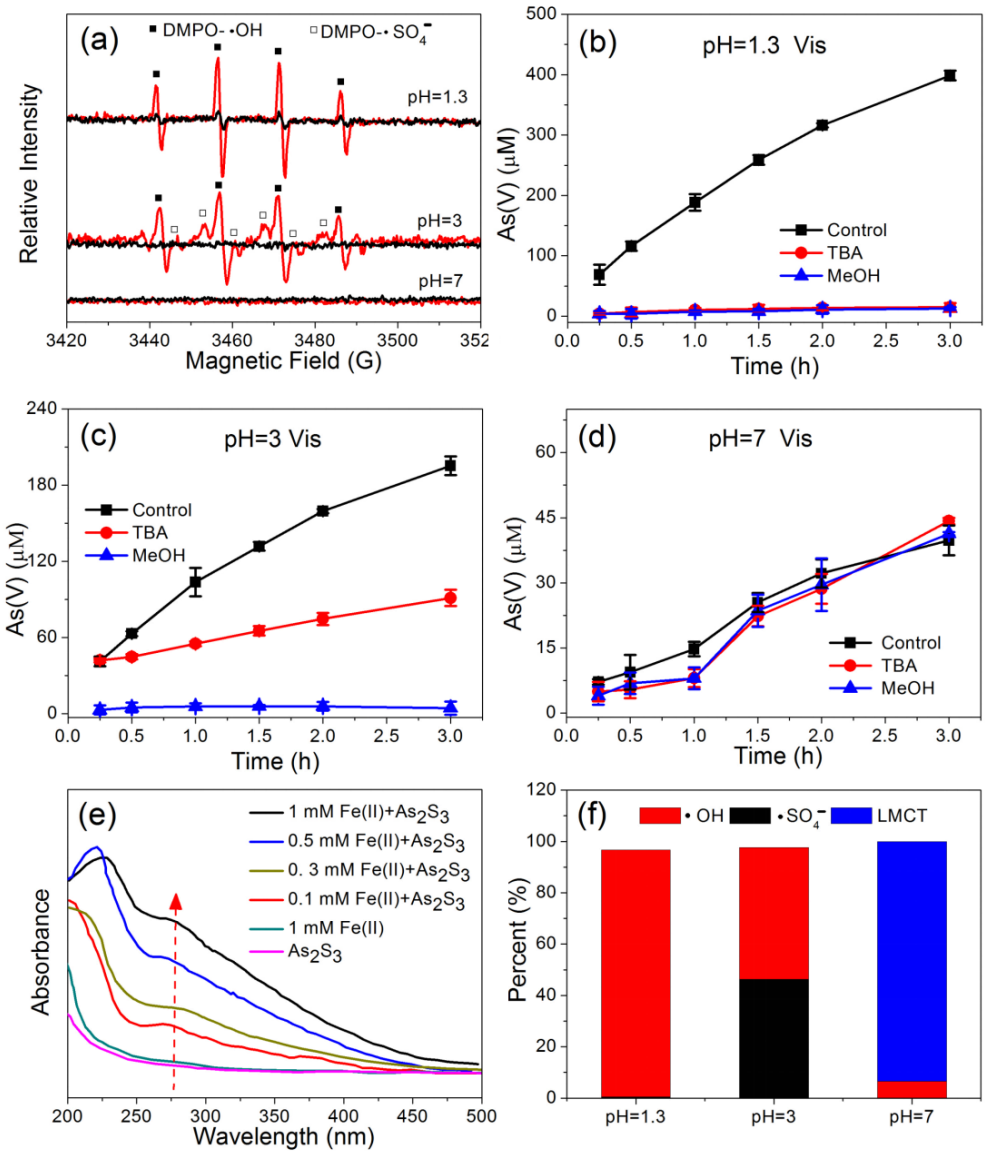

Fig. 4. (a) EPR spectra of DMPO-•OH and DMPO-•SO_4^- detected in As_2S_3 systems with (red lines) and without (black lines) 1 mM Fe(II) at different pHs under visible light. (b-d) Quenching effects of the radical scavengers (TBA and MeOH) on the oxidation of arsenic in the presence of 1 mM Fe(II) at different pHs. (e) UV−vis absorption spectra of CFH−As(III) complex formed in the Fe(II)-As_2S_3 system at pH 7.0 after 1 h of light irradiation. (f) Contribution ratio of the oxidation effect by •OH,

•SO_4^- and LMCT after 3 h of light irradiation at different pHs.

Active free radicals and their effects on the oxidation of arsenic. EPR was used to investigate the photo-generated free radicals in the system of Fe(II)-As_2S_3 under light irradiation. In the dark, no free radical signal was detected both with and without the Fe(II) addition (Fig. S8). Under visible light, in the absence of Fe(II) only a very weak signal of DMPO-•OH[31] was detected at pH 1.3, while no signal was observed at pH 3 and 7 (Fig. 4a). By contrast, in the presence of Fe(II) the signal intensity of DMPO-•OH markedly enhanced at pH 1.3, nearly 10 times higher than that in the absence of Fe(II). At pH 3, besides the characteristic peaks of DMPO-•OH, an obvious signal of DMPO-•SO_4^-[32] was detected. It indicated that Fe(II) did greatly promote the production of free radicals under visible light. However, there were no any free radicals captured at pH 7, although the oxidation of arsenic sulfide was also obtained in the neutral condition (Fig. 2c). The EPR results implied that the mechanism of Fe(II)-promoted free radicals production was pH-depended. On the other hand, DMPO-•O_2^-[33] was detected in all the above systems both with and without Fe(II) under visible light (Fig. S9), where •O_2^- was mainly contributed to the dissolution of As_2S_3 to release As(III) ions via the photochemical reaction (eq. 3), as discussed in our previous work.[12]

In order to verify the effect of the aforementioned free radicals on the oxidation of As_2S_3, the quenchers were employed in the photochemical reaction systems. In the scavenging experiments, TBA was used to capture •OH ($k_{TBA, \cdot OH}$ = (3.8–7.6) × 10^8

M^{-1} s^{-1}), while MeOH was for both •OH and $•SO_4^-$ ($k_{MeOH, •OH}$ =7.8 × 10^8 M^{-1} s^{-1}, $k_{MeOH, •SO_4^-}$= 2.5 × 10^7 M−1 s^{-1}) (Fig. 4b-d). At pH 1.3, both TBA and MeOH completely inhibited the oxidation of arsenic, which indicated only hydroxyl radical contributed to the arsenic oxidation (Fig. 4b). At pH 3, the addition of TBA only partially prohibited the oxidation of As(III) (~51.8% cut) (Fig. 4c). But in the presence of MeOH, the concentration of As(V) was decreased to zero. This indicated that at pH 3, arsenic was oxidized by both hydroxyl radical and sulfate radical.

As no free radicals were detected at pH 7, the addition of TBA and MeOH had no influence to the arsenic oxidation (Fig. 4d). It has been reported that at neutral pH, hydrated Fe(III) oxide could interact with As(III) to form CFH-As(III) complex.[34-36] This was verified in our system, where an increase in UV absorption at 280 nm proved the formation of CFH-As (III) complexes (Fig. 4e).[17,37] Under light irradiation, the oxidation of As(III) can also occur on the surface of CFH-As(III) complexes via photo-induced ligand-to-metal-charge transfer (LMCT).[17] On the basis of quenching results, the contributions of different radicals and non-radicals to the arsenic oxidation at different pHs were summarized in Fig. 4f, where at very acid (pH=1.3) and neutral (pH=7) conditions, •OH and LMCT were exclusively contributed to the oxidation of As(III) in Fe(II)-As_2S_3 system, respectively. At pH=3, •OH and $•SO_4^-$ made almost the equivalent contribution to the oxidation effect.

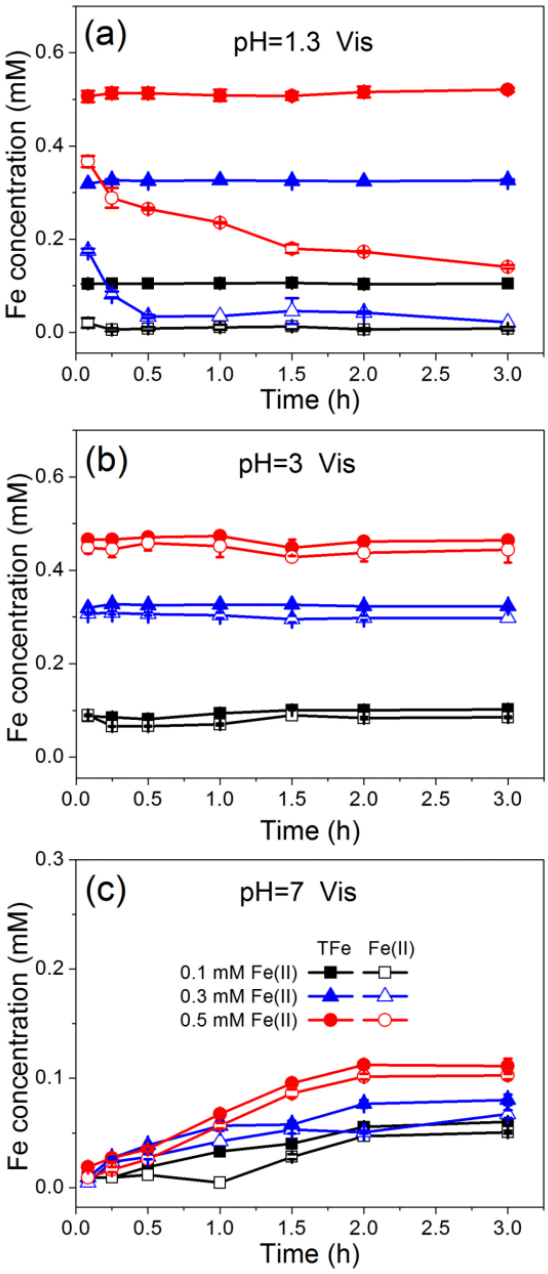

Fig. 5. Variation of iron ions in the system of Fe(II)-As_2S_3 at pH 1.3 (a), 3 (b), and 7 (c) under visible light.

Variation of iron species. In order to disclose the role of iron ions in the photo-oxidation of arsenic sulfide, the variation of iron species in the solution was monitored during the reaction. In the dark, the concentration of Fe(II) almost

remained constant at pH 1.3 and 3 (Fig. S10), and little Fe(III) was detected. This indicated that acidic condition prohibited the oxidation of Fe(II) by dissolved oxygen.[38] At pH 7, the added Fe(II) was not detected in the solution, which might be due to the fact that Fe(II) is easily oxidized to Fe(III) and then precipitated as CFH under neutral conditions (pKsp of $Fe(OH)_3$ = 38.55).[39,40] This was evidenced by the experimental phenomena that the solution rapidly turned orange when adjusting the pH to 7. Under light irradiation (Fig. 5), the concentration of total Fe (TFe) in the solution at pH 1.3 and 3 kept constant as the same amount of Fe(II) initially added. This meant that iron ions were not precipitated or adsorbed at both pH values. But the change of Fe(II) concentration with time behaved completely different at pH 1.3 and 3. At pH 1.3, the concentration of Fe(II) decreased with time. Considering that the total Fe concentration was constant during the reaction, it suggest that Fe(II) was mainly transformed into Fe(III). However, the concentration of Fe(II) at pH 3 was close to that of TFe and hardly change with time, which indicated Fe(II) was the predominant form in this system. The difference of iron species presented at different pHs might be due to the reason that Fe(II) was mainly consumed to produce more hydroxyl radicals at pH 1.3, while more reductive SO_3^{2-} formed at pH 3 can convert Fe(III) back to Fe(II). The mechanism was discussed in detail below.

At pH 7, no Fe ion was detected at the initial time, due to the precipitation of CFH as in the dark case. As the photo-reaction proceeded, the concentration of both Fe(II) and TFe gradually increased, which was probably from the dissolution of the CFH precipitates under light irradiation,[17] although iron(III) still existed mainly in the

form of CFH.

Mechanisms of Fe(II) accelerating the oxidation of As in Fe(II)-As_2S_3 system. From the above results, it can be concluded that the presence of ferrous greatly accelerated the photo-oxidation process of arsenic. In the absence of iron, photocatalysis of arsenic sulfide can also produce superoxide radicals (eqs. 1-2) under visible light.[13] Normally, superoxide radicals could continuously generate hydrogen peroxide and hydroxyl radicals in acid conditions (eqs. 3-4).[41] However, the generation of hydroxyl radicals in the pure As_2S_3 system was very limited (see ESR results in Fig. 4a), probably by the reductive S(II) on the surface of As_2S_3 under visible light (eqs.7-8).[42]

$$\bullet OH + H^+ + S(II)_{(s)} \rightarrow H_2O + \bullet S^-_{(s)} \qquad k=9.0\times10^9\ M^{-1}\ s^{-1} \tag{7}$$

$$2\bullet S^-_{(s)} \rightarrow 1/8S_8 + S^{2-} \qquad k=4.0\times10^9\ M^{-1}\ s^{-1} \tag{8}$$

When Fe(II) was added in the solution, it can act as the catalyst in Fenton-like reactions, leading to a marked increase in the formation of hydrogen peroxide (eq. 9) and hydroxyl radicals (eq. 10).[43,44] On the other hand, Fe(II) ions in the solution can transfer active radicals generated on the particle surface to the solution, preventing the self-consumption by S(II) on the solid As_2S_3. Taking together, the addition of Fe(II) promoted the production of hydroxyl radicals at acid conditions. As a result, the oxidation efficiency of arsenic by hydroxyl radicals was improved (eq. 6).[45,46]

$$HO_2\bullet + Fe(II) + H^+ \rightarrow Fe(III) + H_2O_2 \qquad k=1.2\times10^6\ M^{-1}s^{-1} \tag{9}$$

$$Fe(II) + H_2O_2 \rightarrow Fe(III) + OH^- + \bullet OH \qquad k=1.1\times10^6\ M^{-1}s^{-1} \tag{10}$$

The oxidation of As(III) was overwhelmingly controlled by hydroxyl radicals at

pH 1.3. As the pH value increased to 3, new sulfate radicals were formed via the chain reactions between SO_3^{2-} and Fe(II)/Fe(III),[15] where SO_3^{2-} was originated from the oxidation of S(II) by HO_2• or •OH (eq. 11). First, sulfite combined with Fe(II) or Fe(III) to form Fe(II)-SO_3^{2-} or Fe(III)-SO_3^{2-} complexes, in which Fe(II)-SO_3^{2-} would be further oxidized into Fe(III)-SO_3^{2-} (eqs. 12-14). Then, •SO_3^- was produced from Fe(III)-SO_3^{2-} complex under the activation of light, and was immediately oxidized into •SO_5^- intermediate by dissolved oxygen (eqs. 15-16). Finally, •SO_4^- was generated as the product of the reaction between •SO_5^- and sulfite, and then served for the oxidation of arsenic (eqs. 17-18).[47]

From eqs. 11-18, it can be seen that S(II) was the starting point to trigger the chain reactions between SO_3^{2-} and Fe(II)/Fe(III). Although SO_3^{2-} was hardly detected in the solution, it could be observed on the surface of solid As_2S_3 by XPS spectra (Fig. 3c). Indeed, SO_3^{2-} was detected at pH 3 rather than at pH 1.3, probably because more S(II) can be dissolved from As_2S_3 at the higher pH. As a result, •SO_4^- was obtained at pH 3, instead of pH 1.3. In addition, during the whole process, iron was finally released in the form of Fe(II) in the solution. Thus, Fe(III) precipitation was avoided, which could ensure that the formation efficiency of free radicals was not reduced with time.[14,20]

$$\equiv S(II)+HO_2\bullet/\bullet OH \rightarrow \equiv SO_3^{2-}+S^0+H^+ \quad (11)$$

$$\equiv HSO_3^- + Fe^{2+} \rightarrow FeHSO_3^+ \qquad k=10^{-4}\ M^{-1}\ s^{-1} \quad (12)$$

$$4FeHSO_3^+ + O_2 \rightarrow 4FeSO_3^+ + 2H_2O \qquad \text{fast} \quad (13)$$

$$\equiv SO_3^{2-} + Fe^{3+} \rightarrow FeSO_3^+ \qquad \text{fast} \quad (14)$$

$$FeSO_3^{+} \rightarrow Fe^{2+} + \bullet SO_3^{-} \quad k=0.19\ s^{-1} \tag{15}$$

$$\bullet SO_3^{-} + O_2 \rightarrow \bullet SO_5^{-} \quad k=(1\text{-}2.3)\times10^{9}\ M^{-1}\ s^{-1} \tag{16}$$

$$\bullet SO_5^{-} + HSO_3^{-} \rightarrow SO_4^{2-} + \bullet SO_4^{-} + H^{+} \quad k=10^{4}\text{-}10^{7}\ M^{-1}\ s^{-1} \tag{17}$$

$$\bullet SO_4^{-} + As(III) \rightarrow SO_4^{2-} + As(V) \quad k=6.1\times10^{9}\ M^{-1}\ s^{-1} \tag{18}$$

The radical-involved oxidation process decayed with the increase of pH, due to the precipitation of ferrous or ferric ions. However, Fe(II) was rapidly oxidized to Fe(III) under neutral conditions (pH=7), and generated nascent colloid ferric hydroxide (CFH), which could combine with photo-dissolved As(III) from As_2S_3 to form CFH-As(III).[16] Under light irradiation, an electron transferred from As(III) to Fe(III) on the surface of the CFH−As(III) complex by LMCT mechanism, which will lead to the oxidation of As(III) into As(IV), followed by forming As(V) with the assistant of the oxidation by O_2 or Fe(III) (eqs. 19-22).[17]

$$Fe(OH)_3\text{-}As(OH)_3 + h\nu \rightarrow Fe(OH)_2 + As(OH)_4 \tag{19}$$

$$As(OH)_4 + Fe(OH)_3 \rightarrow As(OH)_5 + Fe(OH)_2 \tag{20}$$

$$2As(OH)_4 \rightarrow As(OH)_5 + As(OH)_3 \tag{21}$$

$$As(OH)_4 + O_2 \rightarrow As(OH)_4^{+} + \bullet O_2^{-} \tag{22}$$

The pH-dependent effect of iron ions on the release and oxidation of As_2S_3 under visible light was summarized in Fig. 6. The addition of Fe(II) exerted little effect on the dissolution and release of As_2S_3. However, Fe(II) can promote the generation of •OH and $\bullet SO_4^{-}$ to accelerate the oxidation of As(III) released from As_2S_3 at acid conditions, while at pH 7, Fe(II) can form CFH to oxidize As(III) by LMCT under visible light.

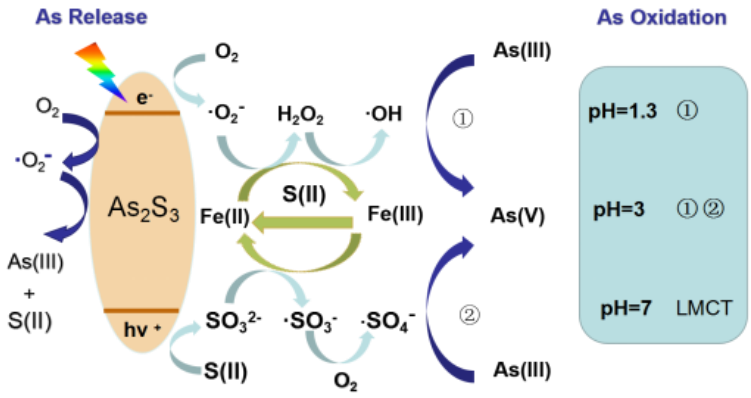

Fig. 6. Schematic illustration of the dissolution and oxidation of As_2S_3 by visible light irradiation in the presence of Fe(II) ions.

Fe(II)/Fe(III) cycling. During the oxidation of As(III), the catalyst, Fe(II), would transform into Fe(III) at acid conditions (eqs. 9-10). While in the photo-reactions of Fe(II)-As_2S_3 system, the byproducts of reductive sulfur species, such as S^{2-}, SO_3^{2-}, and $\bullet SO_3^-$, can make a reversible transition of the oxidative Fe(III) into Fe(II) (eqs. 23-24), and thus keep the Fe(II)/Fe(III) cycling to continuously accelerate the photo-oxidation of As_2S_3. The reversible transition might be more effective at pH 3, where about 94% of Fe ions existed in the form of Fe(II) and kept constant with time.

$$\equiv S(II)/S(II)+2Fe(III)\rightarrow 2Fe(II)+S^0 \quad (23)$$

$$2\equiv SO_3^{2-}+2H_2O+4Fe(III)\rightarrow 4Fe(II)+2SO_4^{2-}+4H^+ \quad (24)$$

In order to verify the Fe(II)/Fe(III) cycling during the photochemical reaction, 1 mM Fe(III), instead of Fe(II), was initially added. Similar to the case of Fe(II)-As_2S_3, the addition of Fe(III) can also obviously increase the generation of As(V) at acid conditions under visible light (Fig. 7a). Accordingly, Fe(III) ions are the main species at pH 1.3, while Fe(II) ions that were reduced from Fe(III) are dominant at pH 3 (Fig. S11). The result further confirmed the effect of Fe(II)/Fe(III) cycling on the oxidation

of As(III), which is independent of the initial redox state of iron ions.

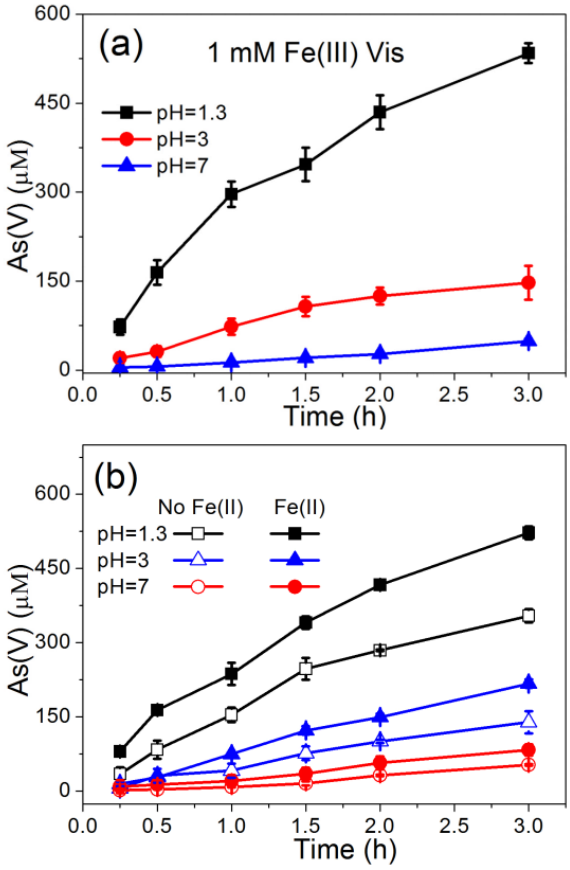

Fig. 7 (a) Oxidation of arsenic in As_2S_3 under visible light in the presence of 1 mM Fe(III). (b) Oxidation of real arsenic sulfide sludge under visible light in the presence of 1 mM Fe(II).

Environmental Implications.

In order to verify the effect of ferrous ions on the real arsenic sulfide sludge, ASS that sampled from a smelting factory in Henan province of China was further examined (Fig. S13). The sludge originally contained 0.8% iron element (Table S3). Without adding extra Fe(II), arsenic in ASS was also oxidized into As(V) under light irradiation at all three pH values (Fig. 7b). However, the oxidation of arsenic was further promoted by the addition of 1mM Fe(II). It verified that iron in ASS played a

crucial role in promoting the photochemical oxidation of arsenic in ASS. Therefore, this study will not only help to understand the transformation and fate of ASS affected by light irradiation and co-existing ions (e.g. ferrous and sulfur-containing ions), but also potentially develop an effective strategy for the safe stocking and treatment of slag residue in industry.

ASSOCIATED CONTENT

Supporting Information

The XRD, SEM, XPS spectra and photos of As_2S_3, the effect of Fe(II) on the XRD and ESR spectra of As_2S_3 with and without visible light irradiation and the effects of dissolved oxygen and Fe(III) on the photo-dissolution and photo-oxidation of As_2S_3. This material is available free of charge via the Internet at http://pubs.acs.org/.

AUTHOR INFORMATION

Corresponding Authors

*Tel: 86-10-62919003; fax: 86-10-62919003; e-mail: jingzhang@rcees.ac.cn.

*Tel: 86-20-39380503; fax: 86-20-39380508; e-mail: zlin@scut.edu.cn.

Notes

The authors declare no competing financial interest.

ACKNOWLEDGMENTS

The authors acknowledge the financial support from National Key Research and Development Program of China (2017YFA0207204 and 2016YFA0203101), the National Natural Science Foundation of China (21876190 and 21836002), the Key

Research and Development Program of Ningxia (2017BY064), and the “One Hundred Talents Program” in Chinese Academy of Sciences.

REFERENCES

1. Kim, D. H.; Bokare, A. D.; Koo, M. S.; Choi, W. Heterogeneous catalytic oxidation of As(III) on nonferrous metal oxides in the presence of H_2O_2. *Environ. Sci. Technol.* **2015,** *49* (6), 3506–3513.

2. Riveros, P. A.; Dutrizac, J. E.; Spencer, P. Arsenic disposal practices in the metallurgical industry. *Can. Metall. Q.* **2001,** *40* (4), 395–420.

3. Jamieson, H. E. The Legacy of Arsenic contamination from mining and processing refractory gold ore at giant mine, Yellowknife, Northwest Territories, Canada. *Rev. Mineral. Geochem.* **2014,** *79*, 533–587.

4. Kong, L. H.; Peng, X. J.; Hu, X. Y. Mechanisms of UV-light promoted removal of As(V) by sulfide from strongly acidic wastewater. *Environ. Sci. Technol.* **2017,** *51* (21), 12583–12591.

5. Lewis, A.; Van Hille, R. An exploration into the sulphide precipitation method and its effect on metal sulphide removal. *Hydrometallurgy* **2006,** *81* (3-4), 197–204.

6. Guo, L.; Du, Y. G.; Yi, Q. S.; Li, D. S.; Cao, L. W.; Du, D. Y. Efficient removal of arsenic from "dirty acid" wastewater by using a novel immersed multi-start distributor for sulphide feeding. *Sep. Purif. Technol.* **2015,** *142*, 209–214.

7. Bhattacharya, A.; Routh, J.; Jacks, G.; Bhattacharya, P.; Morth, M. Environmental assessment of abandoned mine tailings in Adak, Vasterbotten district (northern Sweden). *Appl. Geochem.* **2006,** *21* (10), 1760–1780.

8. Floroiu, R. M.; Davis, A. P.; Torrents, A. Kinetics and mechanism of As_2S_3(am) dissolution under N-2. *Environ. Sci. Technol.* **2004,** *38* (4), 1031–1037.

9. Eary, L. E. The solubility of amorphous As_2S_3 from 25 to 90 ^oC. *Geochim. Cosmochim. Acta.* **1992,** *56* (6), 2267–2280.

10. Lengke, M. F.; Tempel, R. N. Geochemical modeling of arsenic sulfide oxidation kinetics in a mining environment. *Geochim. Cosmochim. Acta.* **2005,** *69* (2), 341–356.

11. Lu, A. H.; Li, Y.; Ding, H. R.; Hochella, M. F. Photoelectric conversion on Earth's surface via widespread Fe- and Mn-mineral coatings. *Proc. Natl. Acad. Sci. U. S. A.* **2019,** *116* (20), 9741–9746.

12. Lu, H. B.; Liu, X. M.; Liu, F.; Hao, Z. P.; Zhang, J.; Lin, Z.; Barnett, Y.; Pan, G. Visible-light photocatalysis accelerates As(III) release and oxidation from arsenic-containing sludge. *Appl. Catal. B-Environ.* **2019,** *250*, 1–9.

13. Mills, G.; Li, Z. G.; Meisel, D. Photochemistry and spectroscopy of colloidal As_2S_3. *J. Phys. Chem. J. Phys. Chem.* **1988**, *92* (3), 822–828.

14. Hug, S. J.; Canonica, L.; Wegelin, M.; Gechter, D.; Von Gunten, U. Solar oxidation and removal of arsenic at circumneutral pH in iron containing waters. *Environ. Sci. Technol.* **2001,** *35* (10), 2114–2121.

15. Xu, J.; Ding, W.; Wu, F.; Mailhot, G.; Zhou, D. N.; Hanna, K. Rapid catalytic oxidation of arsenite to arsenate in an iron(III)/sulfite system under visible light. *Appl. Catal. B-Environ.* **2016,** *186*, 56–61.

16. Ding, W.; Xu, J.; Chen, T.; Liu, C. S.; Li, J. J.; Wu, F. Co-oxidation of As(III) and Fe(II) by oxygen through complexation between As(III) and Fe(II)/Fe(III) species. *Water Res.* **2018,** *143*, 599–607.

17. Xu, J.; Li, J. J.; Wu, F.; Zhang, Y. Rapid photooxidation of As(III) through surface

complexation with nascent colloidal ferric hydroxide. *Environ. Sci. Technol.* **2014,** *48* (1), 272–278.

18. Yu, Y. M.; Zhu, Y. X.; Gao, Z. M.; Gammons, C. H.; Li, D. X. Rates of arsenopyrite oxidation by oxygen and Fe(III) at pH 1.8-12.6 and 15-45 degrees C. *Environ. Sci. Technol.* **2007,** *41* (18), 6460–6464.

19. Wang, X.; Zhang, H.; Wang, L. L.; Chen, J.; Xu, S. Q.; Hou, H. J.; Shi, Y.; Zhang, J. D.; Ma, M.; Tsang, D. C. W.; Crittenden, J. C. Transformation of arsenic during realgar tailings stabilization using ferrous sulfate in a pilot-scale treatment. *Sci. Total Environ.* **2019,** *668*, 32–39.

20. Jiang, X. H.; Xing, Q. J.; Luo, X. B.; Li, F.; Zou, J. P.; Liu, S. S.; Li, X.; Wang, X. K. Simultaneous photoreduction of Uranium(VI) and photooxidation of Arsenic (III) in aqueous solution over g-C_3N_4/TiO_2 heterostructured catalysts under simulated sunlight irradiation. *Appl. Catal. B-Environ.* **2018,** *228*, 29–38.

21. Bai, X. X.; Wang, Y.; Zheng, X.; Zhu, K. M.; Long, A. H.; Wu, X. G.; Zhang, H. Remediation of phenanthrene contaminated soil by coupling soil washing with Tween 80, oxidation using the UV/$S_2O_8^{2-}$ process and recycling of the surfactant. *Chem. Eng. J.* **2019,** *369*, 1014–1023.

22. Hu, S.; Lu, J. S.; Jing, C. Y. A novel colorimetric method for field arsenic speciation analysis. *J. Environ. Sci.* **2012,** *24* (7), 1341–1346.

23. Cline, J. D. Spectrophotometric determination of hydrogen sulfide in natural waters. *Limnol. Oceanogr.* **1969**, *14* (3), 454–458.

24. Humphrey, R. E.; Ward, M. H.; Hinze, W. Spectrophotometric determination of

sulfite with 4,4'-dithiodipyridine and 5,5'-dithiobis-(2-nitrobenzoic acid). *Anal. Chem.* **1970,** *42* (7), 698–702.

25. Tamura, H.; Goto, K.; Yotsuyan.T; Nagayama, M. Spectrophotometric determination of iron(II) with 1,10-phenanthroline in presence of large amounts of iron(III). *Talanta* **1974,** *21* (4), 314–318.

26. Meng, X. G.; Bang, S.; Korfiatis, G. P. Effects of silicate, sulfate, and carbonate on arsenic removal by ferric chloride. *Water Res.* **2000,** *34* (4), 1255–1261.

27. Lu, Y.; Li, J. F.; Li, Y. M.; Liang, L. P.; Dong, H. P.; Chen, K.; Yao, C. X.; Li, Z. F.; Li, J. X.; Guan, X. H. The roles of pyrite for enhancing reductive removal of nitrobenzene by zero-valent iron. *Appl. Catal. B-Environ.* **2019,** *242*, 9–18.

28. Li, Y.; Liang, J.; Yang, Z.; Wang, H.; Liu, Y. Reduction and immobilization of hexavalent chromium in chromite ore processing residue using amorphous FeS_2. *Sci. Total Environ.* **2019,** *658*, 315–323.

29. Scheinost, A. C.; Kirsch, R.; Banerjee, D.; Fernandez-Martinez, A.; Zaenker, H.; Funke, H.; Charlet, L. X-ray absorption and photoelectron spectroscopy investigation of selenite reduction by Fe-II-bearing minerals. *J. Contam. Hydrol.* **2008,** *102* (3-4), 228–245.

30. Sankararamakrishnan, N.; Shankhwar, A.; Chauhan, D. Mechanistic insights on immobilization and decontamination of hexavalent chromium onto nano MgS/FeS doped cellulose nanofibres. *Chemosphere* **2019,** *228*, 390–397.

31. Xu, X.; Lu, R. J.; Zhao, X. F.; Zhu, Y.; Xu, S. L.; Zhang, F. Z. Novel mesoporous $Zn_xCd_{1-x}S$ nanoparticles as highly efficient photocatalysts. *Appl. Catal. B-Environ.*

2012, *125*, 11–20.

32. Dong, X. B.; Ren, B. X.; Sun, Z. M.; Li, C. Q.; Zhang, X. W.; Kong, M. H.; Zheng, S. L.; Dionysiou, D. D. Monodispersed $CuFe_2O_4$ nanoparticles anchored on natural kaolinite as highly efficient peroxymonosulfate catalyst for bisphenol A degradation. *Appl. Catal. B-Environ.* **2019,** *253*, 206–217.

33. Guo, J. G.; Liu, Y.; Hao, Y. J.; Li, Y. L.; Wang, X. J.; Liu, R. H.; Li, F. T. Comparison of importance between separation efficiency and valence band position: The case of heterostructured Bi_3O_4Br/alpha-Bi_2O_3 photocatalysts. *Appl. Catal. B-Environ.* **2018,** *224*, 841–853.

34. Sarkar, S.; Blaney, L. M.; Gupta, A.; Ghosh, D.; Sengupta, A. K. Arsenic removal from groundwater and its safe containment in a rural environment: Validation of a sustainable approach. *Environ. Sci. Technol.* **2008,** *42* (12), 4268–4273.

35. Roberts, L. C.; Hug, S. J.; Ruettimann, T.; Billah, M.; Khan, A. W.; Rahman, M. T. Arsenic removal with iron(II) and iron(III) waters with high silicate and phosphate concentrations. *Environ. Sci. Technol.* **2004,** *38* (1), 307–315.

36. Meng, X. G.; Bang, S.; Korfiatis, G. P. Effects of silicate, sulfate, and carbonate on arsenic removal by ferric chloride. *Water Res.* **2000,** *34* (4), 1255–1261.

37. Pozdnyakov, I. P.; Ding, W.; Xu, J.; Chen, L.; Wu, F.; Grivin, V. P.; Plyusnin, V. F. Photochemical transformation of an iron(III)-arsenite complex in acidic aqueous solution. *Photochem. Photobiol. Sci.* **2016,** *15* (3), 431–439.

38. Stumm, W.; Lee, G. F. Oxygenation of ferrous iron. *Ind. Eng. Chem. Res.* **1961,** *53* (2), 143–146.

39. Stumm, W.; Morgan, J. J. Aquatic Chemistry, Chemical Equilibria and Rates in Natural Waters, 3rd ed.; John Wiley & Sons: NewYork, 1996.

40. Millero, F. J.; Sotolongo, S.; Izaguirre, M. The oxidation kinetics of Fe(II) in seawater. *Geochim. Cosmochim. Acta* **1987,** *51* (4), 793–801.

41. Zhang, Z. H.; Yu, F. Y.; Huang, L. R.; Jiatieli, J.; Li, Y. Y.; Song, L. J.; Yu, N.; Dionysiou, D. D. Confirmation of hydroxyl radicals ((OH)-O-center dot) generated in the presence of TiO_2 supported on AC under microwave irradiation. *J. Hazard. Mater.* **2014,** *278*, 152–157.

42. Das, T. N.; Huie, R. E.; Neta, P.; Padmaja, S. Reduction potential of the sulfhydryl radical: Pulse radiolysis and laser flash photolysis studies of the formation and reactions of center dot SH and HSSH center dot(-) in aqueous solutions. *J. Phys. Chem.* **1999,** *103* (27), 5221–5226.

43. Rush, J. D.; Bielski, B. H. J. Pulse radiolytic studies of the reactions of HO_2/O_2^- with Fe(II)/Fe(III) ions - the reactivity of HO_2/O_2^- with ferric ions and its implication on the occurrence of the haber-weiss reaction. *J. Phys. Chem.* **1985,** *89* (23), 5062–5066.

44. Millero, F. J.; Sotolongo, S. The oxidation of Fe(II) with H_2O_2 in seawater. *Geochim. Cosmochim. Acta* **1989,** *53* (8), 1867–1873.

45. Jiang, B.; Guo, J. B.; Wang, Z. H.; Zheng, X.; Zheng, J. T.; Wu, W. T.; Wu, M. B.; Xue, Q. Z. A green approach towards simultaneous remediations of chromium(VI) and arsenic(III) in aqueous solution. *Chem. Eng. J.* **2015,** *262*, 1144–1151.

46. Ryu, J.; Monllor-Satoca, D.; Kim, D. H.; Yeo, J.; Choi, W. Photooxidation of

arsenite under 254 nm irradiation with a quantum yield higher than unity. *Environ. Sci. Technol.* **2013,** *47* (16), 9381–9387.

47. Woods, R.; Kolthoff, I. M.; Meehan, E. J. Arsenic(IV) as an intermediate in the iinduced oxidation of arsenic(III) by the iron(II)-persulfate reaction and the photoreduction of iron(III). I. absence of oxygen. *J. Am. Chem. Soc.* **1963,** *85* (16), 2385–2390.